

# Non-Zero Syndromes and Syndrome Measurement Order for the $[[7,1,3]]$ Quantum Error Correction Code

Yaakov S. Weinstein<sup>1</sup>

<sup>1</sup>*Quantum Information Science Group, MITRE, 200 Forrester Rd. Princeton, NJ 08540, USA*

The  $[[7,1,3]]$  quantum error correction code uses sets of three syndrome measurements to separately detect bit-flip and phase-flip errors. To comply with the strictures of fault tolerance and thus stem the possible spread of errors to multiple qubits, each set of syndromes is repeated twice. Still, there remains flexibility in the order in which the sets of syndromes are implemented. Here we explore different orders noting that the best choice of syndrome order, determined by the fidelity of the state after noisy error correction, will depend on whether or not an error is detected. To put these results in proper context we first explore the effect on output state fidelity of detecting an error. We find that this fidelity is significantly lower than when no error is detected and may decrease when the single qubit error probabilities decrease.

PACS numbers: 03.67.Pp, 03.67.-a, 03.67.Lx

If quantum computation is to become a reality there must be robust quantum error correction (QEC) codes [1–3]. QEC codes encode a given number of ‘logical’ qubits of quantum information into a larger number of physical qubits. Should one of the physical qubits undergo an error after encoding, measurements of the parity between specified physical qubits, known as syndrome measurements, will locate and identify the error. A recovery operation will then enact the appropriate correction.

QEC forms the backbone of quantum fault tolerance (QFT), the framework that allows for successful quantum computation despite errors in basic computational components [4–7]. The basic concept undergirding QFT is implementing quantum operations in such a way that any error on a single physical qubit will remain localized, *i. e.* the error will not spread to multiple qubits. This can be done by properly designing quantum protocols with the possible use of ancilla qubits, and the repetition of certain protocols in order to relegate errors to second order in error probability. Any remaining single-qubit error can then be corrected by implementing QEC, measuring the syndromes and applying the appropriate recovery operation. By concatenating a QEC code, the probability of a logical qubit error can be suppressed to increasingly higher orders of the physical error probability. An example of a protocol that must be repeated to satisfy the strictures of QFT is the syndrome measurements of the QEC code. Performing the same syndrome measurements twice ensures that errors in the syndrome measurement itself are not causing an improper readout and we can thus rest assured when we apply the signalled recovery operation.

In this work we focus on the order in which the syndrome measurements are performed on quantum information stored in the  $[[7,1,3]]$  or Steane QEC code [8]. The Steane code stores one logical qubit in seven physical, or data, qubits and is the simplest of the CSS codes. There are several methods of syndrome measurement for

the  $[[7,1,3]]$  QEC code compatible with QFT requirements [8, 12]. Here, we utilize four-qubit Shor states [5]. Shor states are simply GHZ states with a Hadamard applied to each qubit. Their construction must also be performed in the nonequiprobable error environment and, following the dictates of QFT, undergo one verification step [13, 14]. Each syndrome measurement then consists of four controlled-NOT (CNOT) gates between the data qubits and Shor state qubits and the parity of the measurements of the Shor state qubits gives the result of the syndrome measurement. Note that no Shor state qubit ever interacts with more than one data qubit thus stemming the spread of any possible error. Three of these syndrome measurements are sufficient to identify the data qubit on which a bit-flip or phase-flip error may have occurred. Thus, in order to locate both bit-flip and phase-flip errors six syndrome measurements are required. The complete QEC process (but with each syndrome measurement set pictured only once) is shown in Fig. 1.

To ensure proper working of the QEC code we enforce that the syndrome measurements be applied as sets, each set containing the three measurements necessary to determine the bit-flip or phase-flip syndrome. Thus, four sets are needed to implement QEC in a fault tolerant fashion. In addition we enforce that the first two sets cannot read out the same type of error and the last two sets cannot read out the same type of error. There are thus four possible syndrome measurement set implementation orders:  $XZXZ$ ,  $XZZX$ ,  $ZXZX$ ,  $ZXZZ$ , where  $X$  ( $Z$ ) refers to the bit-flip (phase-flip) syndrome measurement sets. Our simulations will demonstrate that the optimal choice of syndrome measurement order will depend on whether or not an error is detected. In addition we will see that when an error is detected the fidelity of the output state is significantly lower than when no error is detected and that the fidelity can *increase* when the probability of error increases. All of our simulations are limited to the  $[[7,1,3]]$  QEC code with Shor states for syndrome measurements. Nonetheless, we be-

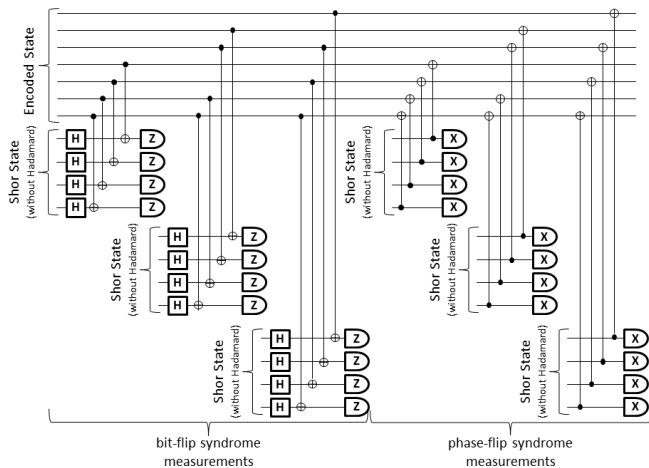


FIG. 1: Fault tolerant bit-flip and phase-flip syndrome measurements for the  $[[7,1,3]]$  code using Shor states (here the Shor states are assumed to have not had the Hadamard gates applied). CNOT gates are represented by  $(\bullet)$  on the control qubit and  $(\oplus)$  on the target qubit connected by a vertical line.  $H$  represents a Hadamard gate. The error syndrome is determined from the parity of the measurement outcomes of the Shor state ancilla qubits. To achieve fault tolerance each of the syndrome measurement sets (bit-flip and phase-flip) is repeated twice (but not twice in a row).

lieve that our demonstration highlights the importance of syndrome measurement order which may be an important issue for other syndrome measurement methods, other CSS codes in general, and for non-CSS codes as well.

We start with an initial encoded state that has been subject to a non-equiprobable error environment. Let  $|\psi(\alpha, \beta)\rangle = \cos\alpha|0\rangle + e^{i\beta}\sin\alpha|1\rangle$  be the wave function of an arbitrary single-qubit pure state and  $\rho_1(\alpha, \beta) = |\psi(\alpha, \beta)\rangle\langle\psi(\alpha, \beta)|$  be the corresponding density matrix. Perfect encoding of this state onto the 7 physical, data qubits appropriate for the Steane code lead to the state  $\rho(\alpha, \beta)$ . We assume a noisy encoding leading to an initial error state that is a mixed density matrix of all possible one qubit errors:

$$\rho_e(\alpha, \beta) = (1 - 7 \sum_j^{x,y,z} p_j) \rho(\alpha, \beta) + \sum_i \sum_j^{x,y,z} p_j \sigma_j^i \rho(\alpha, \beta) \sigma_j^i. \quad (1)$$

Perfectly implemented QEC will correct this error and output the state  $\rho(\alpha, \beta)$ . Noisy QEC leads to an imperfect output state  $\rho_o$ . To determine the accuracy of this output state we utilize physical and logical state fidelities. The physical state fidelity is simply  $F(\rho, \rho_o) = \text{Tr}[\rho\rho_o]$ . To calculate the logical state fidelity we decode  $\rho_o$  and trace out all qubits but the first. This leaves a one qubit state  $\rho_o^{dec}$ . The logical state fidelity is then  $F(\rho_1, \rho_o^{dec}) = \text{Tr}[\rho_1\rho_o^{dec}]$ . The former fidelity measure provides an accuracy measure for the entire evolutionary process of the physical qubits. It also informs us of the fragility of the

physical state from which we can judge the harm a future error will do to the logical information. The latter fidelity measure is the accuracy of the encoded logical information. We will find it useful to utilize the physical and logical state infidelity  $I = 1 - F$ , and a logarithmic infidelity  $-\log_{10}[I]$ . Unless otherwise noted we will utilize the initial state  $\alpha = \beta = 0$ . The fidelity for other states are similar to those reported except for where explicitly stated.

The noise environment for our simulations will be the nonequiprobable Pauli operator error environment [9]. As in [10], this model is a stochastic version of a biased noise model that can be formulated in terms of Hamiltonians coupling the system to an environment. In the model used here the probabilities with which the different error types take place is left arbitrary: qubits undergo a  $\sigma_x^j$  error with probability  $p_x$ , a  $\sigma_y^j$  error with probability  $p_y$ , and a  $\sigma_z^j$  error with probability  $p_z$ , where  $\sigma_i^j$ ,  $i = x, y, z$  are the Pauli spin operators on qubit  $j$ . We assume that qubits taking part in a gate operation, initialization or measurement will be subject to error and that errors are completely uncorrelated. Qubits not involved in a gate are assumed to be perfectly stored. This idealization is partially justified in that it is generally assumed that idle qubits are less likely to undergo error than those involved in gates (see for example [11]).

We first explore the case when the syndrome sets are applied in the order  $XZXZ$  and highlight the contrast between not detecting an error and detecting an error. To model realistic systems we simulate all 1000 permutations for the error probabilities  $p_x = 10^{-m}$ ,  $p_y = 10^{-n}$ , and  $p_z = 10^{-q}$  for  $m, n, q = 1, 2, \dots, 10$ . These simulations will also allow us to compare a nonequiprobable error environment to an equiprobable (or depolarizing) error environment. The logarithmic infidelities as a function of the error probabilities for the case that  $p_z = 10^{-10}$  are shown in the subplots of Fig. 2. Each subplot is for a different error detection outcome: no error, bit-flip error on the first qubit ( $\sigma_x^1$ ), both a bit-flip and phase flip error on the first qubit ( $\sigma_y^1$ ), and a phase-flip error on the first qubit ( $\sigma_z^1$ ).

When no error is detected the fidelity of the output state decreases steadily as the error probability increases as shown in Fig. 2. The rate of logarithmic infidelity decrease is directly proportional to the increase of maximum error probability: when the maximum error probability is increased by an order of magnitude, the logarithmic infidelity decreases by one. When an error probability that is not the maximum is increased, the logarithmic fidelity remains practically constant. The inset shows that the initial decrease in logarithmic infidelity is greater for bit-flip errors (dashed line) than for phase-flip errors or for  $\sigma_y$  errors, both phase-flip and bit-flip errors, (chained line) due to initial transitory behavior. After this the rate of decrease is about the same. How-

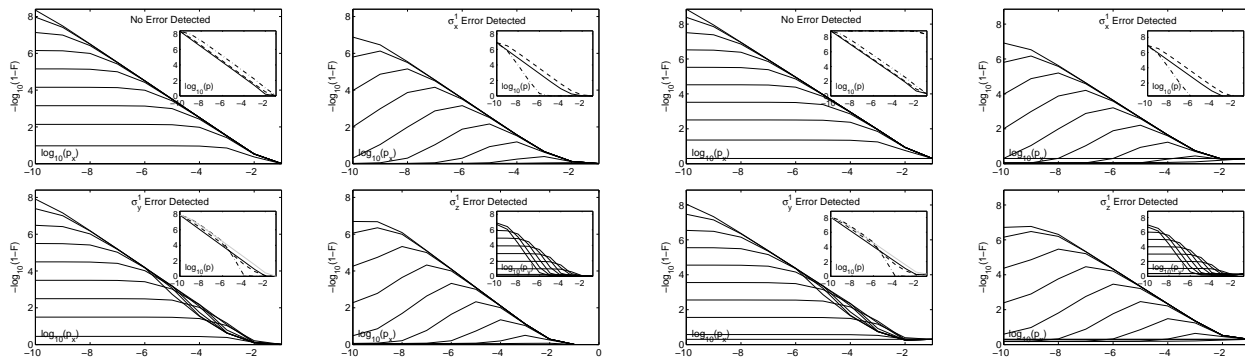


FIG. 2: The four left side plots show the logarithmic infidelity of the physical output state,  $\rho_o$  after QEC on the state  $\rho_e(0, 0)$  when no error is detected, a  $\sigma_x^1$  error is detected, a  $\sigma_y^1$  error is detected, and after QEC on the state  $\rho_e(2.5595, 0.39894)$  when a  $\sigma_z^1$  error is detected as a function of  $p_x$ . Here we have used the syndrome order  $XZXZ$ . Each individual curve is for a different value of  $n$  where  $p_y = 10^{-n}$ , and  $n$  ranges from 1 (bottom curve) to 10 (top curve). For all curves  $p_z$  is set to  $10^{-10}$ . The insets of the first three subplots compare the logarithmic infidelity of the state in a depolarizing environment (solid line) versus environments where bit-flip (dashed line), phase-flip (chain line), or both (same as phase-flip error except for when  $\sigma_y^1$  is detected in which case shown by grey line) environments are dominant. The inset in the  $\sigma_z^1$  error detected subplot displays the logarithmic infidelity as a function of  $p_y$  with  $p_x$  set to  $10^{-10}$ . Each individual curve is for different values of  $q$  where  $p_z = 10^{-q}$ , and  $q$  ranges from 1 (bottom curve) to 10 (second highest curve, the highest curve is for  $q = 9$ ). The four right side plots show the logarithmic infidelity of the logical single-qubit output state,  $\rho_o^{dec}$  after QEC. The behaviors are qualitatively similar to that of the physical state logarithmic infidelities.

ever, if the error types are equiprobable (a depolarizing channel,  $p_x = p_y = p_z = p$ ) the transitory behavior is absent and the logarithmic infidelity under this channel is thus lower than in an environment in which any one error probability is dominant.

When an error is detected and corrected we find that the infidelity of the output is higher than when no error is detected by almost an order of magnitude. Most interestingly, in certain cases an increase in error probability can lead to an increase in output state fidelity. Let us look carefully at this behavior. If a bit-flip error is detected in a depolarizing environment we find that the output physical state logarithmic infidelity is lower than when no error is detected by 1.47 and the logical state logarithmic infidelity is lower by 1.94 for  $p < 10^{-4}$ . In addition, unlike in the case where no error is detected, a depolarizing error can lead to a higher fidelity than when only one of the error probabilities is reduced. For example, the inset of the upper right subplot of Fig. 2 compares the decrease in logarithmic infidelity for a depolarizing environment as a function of  $p$  (solid line) with the decrease of logarithmic infidelity as a function of  $p_x$  (dashed line) and  $p_z$  (chained line) when the other two error probabilities are  $10^{-10}$  (the case of changing  $p_y$  with  $p_x = p_z = 10^{-10}$  gives the same results as changing  $p_z$ ). Clearly, error correction when a bit-flip error is detected works better in the depolarizing case than in the case when  $p_y$  or  $p_z$  are dominant. When the errors are nonequiprobable we notice that increasing the probability of the bit-flip errors, the error type that is in fact detected, increases the infidelity by up to almost three orders of magnitude.

If a  $\sigma_y$  error is detected in a depolarizing environment we find that the output physical state logarithmic infidelity is lower than when no error is detected by 0.44 and the logical state logarithmic infidelity is lower by 0.81 for  $p < 10^{-4}$ . We also find interesting results when comparing the depolarizing environment with environments in which one of the error probabilities is dominant. The depolarizing environment gives the lowest output state fidelity until the logarithmic fidelity is about 5.5. At that point the logarithmic infidelity of the bit-flip and phase-flip dominant errors fall below that of the depolarizing channel. Compared to when  $\sigma_y$  errors are dominant however, the depolarizing channel always gives a lower fidelity. These results are shown in Fig. 2. The main part of the subplot again demonstrates that when an error is detected a higher error probability of the detected error translates to a higher output state fidelity. This is seen by the crossing of the constant  $p_y$  curves. Increasing the bit-flip or phase-flip error probabilities, however, will not lead to a higher fidelity.

If a phase-flip error is detected in a depolarizing environment we find that the output physical state logarithmic infidelity is lower than when no error is detected by 0.91 and the logical state logarithmic infidelity is lower by 0.59 for  $p < 10^{-4}$ . Like the case of the bit-flip detection, the fidelity of the output state after error correction is higher in a depolarizing environment than in an environment where  $\sigma_y$  errors are dominant but lower than in an environment where bit-flip or phase-flip errors are dominant (dominant bit-flip errors give the highest fidelity). When errors are nonequiprobable increasing error prob-

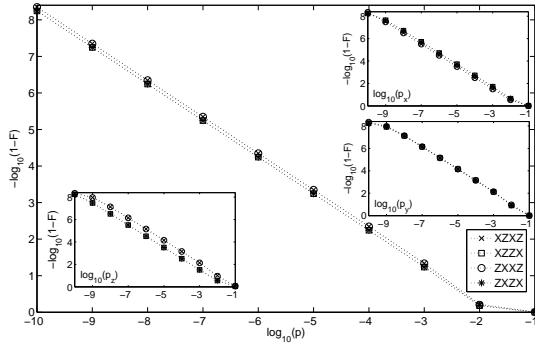


FIG. 3: Fidelity of post QEC state for a depolarizing channel as a function of  $p$  for the different syndrome orders when no error has been detected. In this case  $XZZX$  and  $ZXXZ$  have slightly higher fidelities than the other two syndrome orders. The insets show the fidelity as a function of  $p_i$  given that  $p_j = p_k = 10^{-10}$ , where  $i = x$  (upper right),  $i = y$  (middle right), and  $i = z$  (lower left). As a function of  $p_x$  the syndrome orders  $ZXXZ$  and  $XZZX$  are slightly higher, as a function of  $p_y$  the fidelity is practically independent of the order, and as a function of  $p_z$  the syndrome orders  $XZZX$  and  $ZXXZ$  give the higher fidelity.

ability again leads to higher fidelities.

However, the phase-flip error does not affect the single-qubit state  $\alpha = 0, \beta = 0$  causing the logical state fidelity of  $\rho_\sigma^{dec}$  to be extremely insensitive to phase-flip errors. Fig. 2 thus shows results for the randomly chosen state  $\rho_e(2.5595, 0.39894)$ . Similar to when other error types are detected, we see that as the error probability of the detected error (phase-flip) increases so does the fidelity and, in addition, even when the bit-flip error probability increases so does the fidelity. This is consistent with the results of ?? which shows that bit-flip errors in Shor state construction leads to phase-flip errors in the data qubits.

We now explore the effect of the syndrome set order on the output state fidelity. We again utilize the initial state  $\rho_e$  with  $\alpha = \beta = 0$  and the above used noisy environment with nonequiprobable errors: bit-flip, phase-flip, and both. As above, we will find that the fidelity as a function of the syndrome order will depend on whether or not an error has been detected. Some results for the case where no error is detected are plotted in Fig. 3. As above, we find that the physical and logical state fidelities exhibit qualitatively the same behavior and thus choose to display only the physical state fidelity. The main figure shows the fidelity of the post QEC output state for a depolarizing error environment  $p_x = p_y = p_z = p$  and the three insets are for the cases where two of the error probabilities are kept constant at  $10^{-10}$  and the other increases. In a depolarizing environment or when phase-flip errors are dominant we see that the syndrome orders  $XZZX$  and  $ZXXZ$  give slightly higher fidelities than the other syndrome orders. The syndrome orders

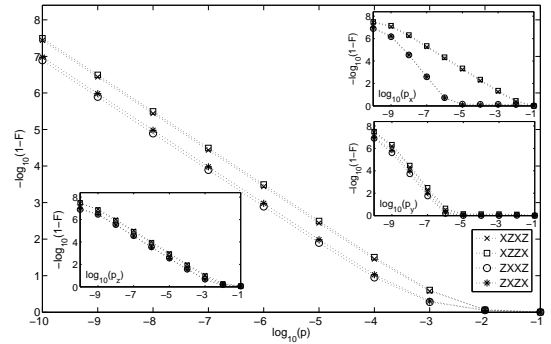


FIG. 4: Fidelity of post QEC state for a depolarizing channel as a function of  $p$  for the different syndrome orders when a phase-flip error on the first qubit has been detected. In this case  $XZZX$  and  $XZXZ$  have slightly higher fidelities than the other two syndrome orders. The insets show the fidelity as a function of  $p_i$  given that  $p_j = p_k = 10^{-10}$ , where  $i = x$  (upper right),  $i = y$  (middle right), and  $i = z$  (lower left). As a function of  $p_x$  the syndrome orders  $XZZX$  and  $XZXZ$  are significantly higher, as a function of  $p_y$  the fidelity is practically independent of the order, and as a function of  $p_z$  the syndrome orders  $XZZX$  and  $ZXXZ$  give the higher fidelity.

$ZXXZ$  and  $XZZX$  are slightly better when bit-flip errors are dominant, and all syndrome orders give about the same fidelity when  $\sigma_y$  errors are dominant.

When a phase flip error is detected on the first qubit the syndrome  $XZZX$  gives the highest fidelity in all of the explored environments followed closely by  $XZXZ$ . The other two syndrome orders give lower fidelities, significantly so when bit-flip errors are dominant. This may be because for both of these syndrome orders a phase flip syndrome measurement, which detects the error, is second out of the four syndromes. The second syndrome measurement completes one full error correction procedure (the second full procedure is implemented afterwards to conform with the strictures of QFT). As we will see the opposite syndrome orders provide better fidelity for the case where bit-flip errors are dominant.

When a bit-flip error is detected on the first qubit the syndrome  $ZXXZ$  gives the highest fidelity for all of the error environments followed closely by  $ZXXZ$ . The other two syndromes give lower fidelities. As in the case when the phase-flip error is detected, the syndrome orders giving the higher fidelities are those with the syndrome measurement for the detected error in the second slot.

When both a phase-flip and bit-flip error are detected on the first qubit which syndrome order gives the best fidelity now depends on which error is dominant. In a depolarization environment or when phase-flip errors are dominant the syndrome order  $ZXXZ$  gives the highest fidelity, followed by  $ZXXZ$ . When  $\sigma_y$  errors are dominant, however,  $ZXXZ$  gives a slightly higher fidelity.

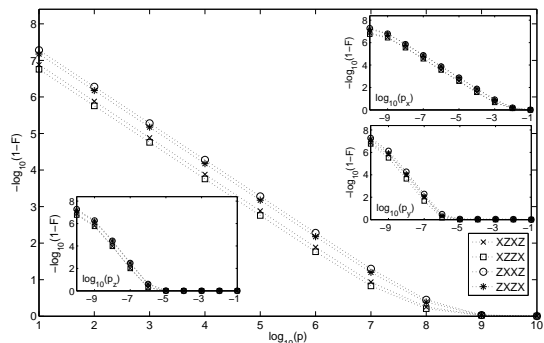


FIG. 5: Fidelity of post QEC state for a depolarizing channel as a function of  $p$  for the different syndrome orders when a bit-flip error on the first qubit has been detected. In this case  $ZXXZ$  and  $ZXZX$  have slightly higher fidelities than the other two syndrome orders. The insets show the fidelity as a function of  $p_i$  given that  $p_j = p_k = 10^{-10}$ , where  $i = x$  (upper right),  $i = y$  (middle right), and  $i = z$  (lower left). As a function of any of these the syndrome orders  $ZXXZ$  and  $ZXZX$  are give the higher fidelity.

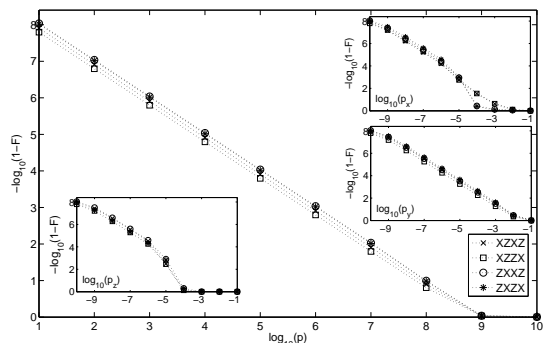


FIG. 6: Fidelity of post QEC state for a depolarizing channel as a function of  $p$  for the different syndrome orders when a  $\sigma_y$  (bit-flip and phase-flip) error on the first qubit has been detected. In this case  $ZXXZ$  and  $ZXZX$  have slightly higher fidelities than the other two syndrome orders. The insets show the fidelity as a function of  $p_i$  given that  $p_j = p_k = 10^{-10}$ , where  $i = x$  (upper right),  $i = y$  (middle right), and  $i = z$  (lower left). As a function of any of these the syndrome orders  $ZXXZ$  and  $ZXZX$  are give the higher fidelity.

When bit-flip errors are dominant the syndrome order with the highest fidelity will depend on the strength of the bit-flip errors.

To further explore the efficiencies of the different syndrome measurement orders we apply QEC 50 times once after each of 50 single logical qubit gates performed in the nonequiprobable error environment on the initial state  $|0\rangle$ . The 50 gates are represented by the composite gates  $A = HST$  and  $B = HT$ , where  $H$  is the Hadamard gate,  $S$  is a phase gate, and  $T$  is the  $\pi/4$  phase gate. These gates are simulated as described in [15]. The 50 gates

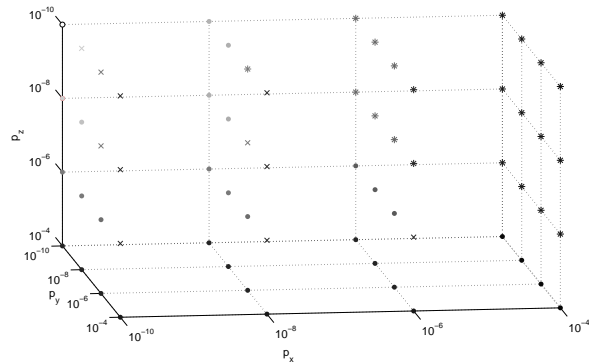


FIG. 7: The marker at every point represents which syndrome order gives the highest fidelity (the markers are the same as in previous figures) for the error environment represented by the three axes. In addition, the lighter the color of the marker the higher the logarithmic infidelity.

are then given by  $ABBBAAAABBABABBBBBAA$ . In these simulations, no error is detected for any of the 50 QEC applications. Figure 7 shows which syndrome order gives the highest output state fidelity for different single-qubit error probabilities. In addition, the lighter the marker the higher the fidelity such that the white marker (upper left corner) represents a logarithmic infidelity of 8.35 and the black marker represents a logarithmic infidelity of 2.31.

For most of the error environments the syndrome order  $ZXXZ$  gives the highest fidelities especially when phase flip errors are dominant. However, when bit flip errors are dominant the syndrome order  $ZXZX$  tends to give the highest fidelities. And, when  $\sigma_y$  errors are dominant the syndrome order  $XZXZ$  gives the highest fidelity. We note that as in the case of one application of QEC, the difference between the best fidelity and second best fidelity tends to be slight, especially between the syndrome order pairs  $ZXXZ$  and  $XZXZ$ , and  $ZXZX$  and  $XZZX$ . Thus, while for some error environments choosing a suboptimal syndrome order may lead to a difference in logarithmic infidelity of up to 0.65, for other suboptimal choices the difference is much less.

In conclusion we have explored the effects of measuring a non-zero syndrome and the syndrome measurement order on the output fidelity of a state encoded into the  $[[7,1,3]]$  quantum error correction code. We have seen that when an error is detected the fidelity may behave in a non-intuitive fashion. For example, the fidelity will increase when error probabilities increase. In addition, symmetric noise (the depolarizing channel) will respond better to error correction than environments with non-equiprobable noise though the total error probability is greater in the depolarizing channel.

The optimal choice of syndrome order also depends on whether or not an error is detected and on what error type is dominant. When no error is detected the

optimal choice of syndrome order will depend on which error probability is dominant. Our simulations suggest that the better syndrome orders will be the ones where the dominant error is measured by the syndrome in the fourth slot. When an error is detected the better working syndromes are those where the detected error is in the second slot of the syndrome order.

While this work is localized to the  $[[7,1,3]]$  code where syndrome measurement is performed by Shor states, similar studies should be conducted for other means of syndrome measurement and other CSS codes in order to optimize quantum computations as much as possible. Optimization of non-CSS codes would also require a similar study.

This research is supported under MITRE Innovation Program Grant 51MSR662. ©2013 - The MITRE Corporation. All rights reserved. Approved for Public Release 13-4069; Distribution Unlimited.



[1] M. Nielsen and I. Chuang, *Quantum information and Computation* (Cambridge University Press, Cambridge,

- 2000).
- [2] P.W. Shor, Phys. Rev. A **52**, R2493 (1995).
- [3] A.R. Calderbank and P.W. Shor, Phys. Rev. A **54**, 1098 (1996);
- [4] J. Preskill, Proc. Roy. Soc. Lond. A **454**, 385 (1998).
- [5] P.W. Shor, *Proceedings of the the 35th Annual Symposium on Fundamentals of Computer Science*, (IEEE Press, Los Alamitos, CA, 1996).
- [6] D. Gottesman, Phys. Rev. A **57**, 127 (1998).
- [7] P. Aleferis, D. Gottesman, and J. Preskill, Quant. Inf. Comput. **6**, 97 (2006). A.M. Steane, Phys. Rev. Lett. **77**, 793 (1996).
- [8] A.M. Steane, Proc. Roy. Soc. Lond. A **452**, 2551 (1996).
- [9] V. Aggarwal, A.R. Calderbank, G. Gilbert, Y.S. Weinstein, Quant. Inf. Proc. **9**, 541 (2010).
- [10] P. Aliferis and J. Preskill, Phys. Rev. A **78**, 052331 (2008).
- [11] K.M. Svore, B.M. Terhal, D.P. DiVincenzo, Phys. Rev. A **72**, 022317 (2005).
- [12] A.M. Steane, Phys. Rev. Lett. **78**, 2252 (1997).
- [13] Y.S. Weinstein, Phys. Rev. A **84**, 012323 (2011).
- [14] Y.S. Weinstein and S.D. Buchbinder, Phys. Rev. A **86**, 052336 (2012).
- [15] Y.S. Weinstein, arXiv:1305.2763 (2013).